
Towards a Generalist and Blind RGB-X Tracker

Yuedong Tan¹ **Zongwei Wu¹** **Yuqian Fu²** **Zhuyun Zhou¹** **Guolei Sun²**
Chao Ma³ **Danda Dani Paudel⁴** **Luc Van Gool^{2,4}** **Radu Timofte¹**
¹University of Würzburg ²CVL, ETH Zürich
³AI Lab, Shanghai Jiao Tong University ⁴INSAIT, Sofia University

Abstract

With the emergence of a single large model capable of successfully solving a multitude of tasks in NLP, there has been growing research interest in achieving similar goals in computer vision. On the one hand, most of these generic models, referred to as generalist vision models, aim at producing unified outputs serving different tasks. On the other hand, some existing models aim to combine different input types (aka data modalities), which are then processed by a single large model. Yet, this step of combination remains specialized, which falls short of serving the initial ambition. In this paper, we showcase that such specialization (during unification) is unnecessary, in the context of RGB-X video object tracking. Our single model tracker, termed XTrack, can remain blind to any modality X during inference time. Our tracker employs a mixture of modal experts comprising those dedicated to shared commonality and others capable of flexibly performing reasoning conditioned on input modality. Such a design ensures the unification of input modalities towards a common latent space, without weakening the modality-specific information representation. With this idea, our training process is extremely simple, integrating multi-label classification loss with a routing function, thereby effectively aligning and unifying all modalities together, even from only paired data. Thus, during inference, we can adopt any modality without relying on the inductive bias of the modal prior and achieve generalist performance. Without any bells and whistles, our generalist and blind tracker can achieve competitive performance compared to well-established modal-specific models on 5 benchmarks across 3 auxiliary modalities, covering commonly used depth, thermal, and event data. The code and models will be available at <https://github.com/supertyd/XTrack>.

1 Introduction

Artificial General Intelligence (AGI), which aims at achieving a generalist model with the ability to understand, learn, and apply knowledge across a wide range of tasks, has recently gained significant research attention [6, 44, 33, 46]. In the realm of Natural Language Processing (NLP), a bunch of flagship generalist models [12, 42, 55, 41] capable of handling various tasks have been proposed. However, AGI’s progress in computer vision remains comparatively less advanced [46, 64, 5]. Recent advancements in multi-modal vision models, which integrate and process data from multiple sensor modalities, have shown promising potential in improving the generalization ability of vision models [36, 15]. Particularly, the RGB-X video object tracking [66, 53, 47] which naturally involves multi-modal inputs and requires the model to predict a unified output is a very typical exemplar for building such multi-modal vision models. Thus, in this paper, we aim to build a generalist model for the RGB-X video object tracking task further pushing the research boundary.

RGB-X video object tracking involves the continuous tracking of objects in video sequences using multi-modal data, based on the input RGB images combined with additional modalities (X) such as depth [51], event [45], and thermal data [32]. RGB, which carries the majority of the visual

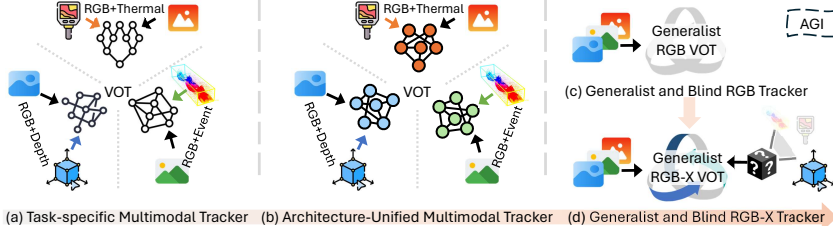


Figure 1: **Motivation:** There have been some more-or-less foundation trackers for RGB VOT. However, current works on RGB-X trackers are still far away from the ultimate goal, since they leverage modality-specific architecture and/or parameters. Differently, we aim for a generalist RGB-X tracker, with one single parameter set and without the need to know the modal prior.

information, is the most basic and important modality, while other modalities serve as supplementary aids. For example, depth information can help address occlusion issues [18, 52], thermal images can provide valuable cues in low-light conditions [60, 63], and event data can enhance motion sensitivity [58, 69]. This combination of these various modalities enhances the robustness and accuracy of object tracking in various challenging scenarios. The inherent complexity of handling multiple modalities and the practical importance of this task make it an ideal candidate for testing and advancing AGI capabilities in multi-modal visions.

Several efforts have been made to promote RGB-X video object tracking, including works such as [53, 66, 47, 67, 51, 57, 14]. Among them, early works often adopt task-specific designs, where the learning modules are tailored for one particular modality [51, 14], as shown in Fig.1(a). Recently, some works have achieved architecture unification [53, 66], while still requiring multiple sets of parameters to handle different modalities and need prior knowledge of the input modality as in Fig.1(b). From our perspective, such a reliance on prior modality knowledge fails to align with the principal expectation of AGI. We believe a good generalist model should be able to autonomously recognize and process different input modalities without any prior indication. Such an AGI tracker has more-or-less achieved in RGB VOT domain. As shown in Fig.1(c), current RGB trackers only require one single parameter but can deal with any input from any dataset and any setting. This motivates us to propose our single and unified model tracker, termed XTrack. As illustrated in Fig.1(d), our XTrack uses a unified architecture with one single parameter set for different modalities. Most importantly, our XTrack could remain blind to any modality X during the inference stage, which we believe can be the right path towards AGI for RGB-X tracking.

Essentially, to achieve the generalist and blind tracker, our key ideas behind XTrack lie in: 1) reformulating all the input modalities as a single-blind input X; 2) disentangling the modality-shared features and modality-specific features. In other words, regardless of whether its actual modality is depth, thermal, or event, we treat it equally as X and input X into our unified model. To fully explore the X, two different types of features are extracted. One is the modality-shared features, which capture common information across various modalities; The other is the modality-specific features, which represent unique cues specific to each modality, such as the geometry from depth, temporal information from thermal, and motion from the event data. Technically, a novel mixture of model experts (MeME) together with a dynamic routing system is proposed to achieve these two objectives, resulting in our XTrack method.

Concretely, our MeME contains a shared expert and several domain-specific experts. The shared expert is responsible for extracting modality-shared features, while the domain-specific experts obtain modality-specific features. Additionally, a router is included in MeME to determine which expert should be used for the current modality X, automatically recognizing the modality type for X. Based on the router’s prediction, we can forward X to its corresponding expert to obtain its modality-specific features. The final feature is a combination of the modality-shared features and the modality-specific features. In this way, we achieve cross-modal unification through joint embedding, while preserving modality-specific clues. Notably, the training of our model is extremely simple: we directly employ a multi-label classification loss to supervise the selection of the most appropriate experts. Finally, the learned generalist knowledge is used to prompt the RGB foundation tracker.

Extensive studies are performed to show the effectiveness of our XTrack, which outperforms established modal-specific models by leveraging a unified set of parameters, viewing the multi-modal system holistically. Our generalist XTrack maintains efficiency with less than 10% modality-aware tuning parameters over our RGB baseline while achieving a tolerable performance degradation of less than 1% compared to the absolute state-of-the-art, i.e., modality-specific trackers.

2 Related Work

There are extensive surveys on the generalist vision models [16, 2, 56, 37]. In this section, we focus exclusively on related RGB-X tracking works, aiming to narrow the gap towards AGI.

Multi-Modal Tracking: In the evolution of object tracking [62, 10, 8, 65], the model architecture has undergone a continuous transformation, transitioning from correlation filters [24, 19] to Siamese networks [8, 17], and then to the current transformer architecture [7, 35] that integrates unified feature extraction and interaction. However, the performance and stability of object tracking are still constrained by the insufficiency of RGB information. Multi-modal information, including depth [18, 52], event [58, 69], and thermal data [60, 63], can compensate for this deficiency and enhance the robustness of object tracking networks. BAT [3] and TBSI [22] have designed a dual-Transformer architecture specifically for RGBT object tracking, while DepthTrack [51] is tailored for RGBD object tracking. Existing multi-modal object tracking algorithms predominantly follow the design paradigm of prompt learning, aiming to establish a unified object tracking paradigm [66, 21, 20, 47, 53] that integrates the model architecture for multi-modal object tracking. However, learning modality-specific parameters is not the right path toward AGI. This drives us to consider downstream modalities as auxiliary means to holistically improve tracking performance.

Multi-Task Learning: Multi-task learning [4] enables different tasks to be processed through a single network. Current research primarily focuses on integrating multiple tasks, with each task having its dedicated tokenizer and task-specific parameters. The Meta-Transformer [61] aligns various modalities into a unified feature space, while ImageBind [15] uses images to align data from different modalities. PolyViT [34] has pioneered the unified training of a Vision Transformer (ViT) backbone using multiple modal data. Although these works have achieved partial unification, they still require different parameters for input and output due to the distinct nature of the tasks being processed. In multi-modal object tracking, the different input modalities are all image-based, and the tasks being addressed are consistent. Therefore, in this paper, we explore a novel approach that models images from different modalities, allowing for the maintenance of uniform parameters across different modal inputs without the need for any task-specific parameters, thereby accomplishing a single task.

Mixture-of-Experts: Mixture of Experts (MoE) has emerged as a powerful technique, enhancing model capability and efficiency by delegating tasks to multiple expert networks. This model architecture is particularly suited for handling complex and diverse data, as it dynamically selects the most appropriate expert based on the characteristics of the input data. Models such as VMoE [39] and DAMeX [23] have significantly improved image classification and object detection tasks by extending the feed-forward network (FFN) layers within the vision transformer architecture. These models dynamically adjust the combination of their internal expert networks based on the features of the input images, thereby capturing complex patterns more effectively. DeepSeekMoE [9] exemplifies the application of MoE in large language models, significantly enhancing language understanding and generation through the expert mixture mechanism. This model selects the most suitable expert network based on the semantics and context of the input text, thus improving the accuracy and efficiency of language processing. Models like IMP [1] and LiMoE [38] leverage MoE to unify tasks across different modalities, such as visual, auditory, and textual data processing. These models share and transfer knowledge across different modalities, thereby enhancing the performance of multi-modal tasks. However, existing MoE algorithms still face challenges in achieving effective division of labor among experts. In this paper, we propose a novel approach that unifies not only the feature extraction part across different modalities but also the input part. This means that regardless of the modality of the input data, the model can effectively process it through the MoE expert mechanism. Additionally, we introduce a constraint mechanism to ensure a clear division of labor among experts.

3 Method

The core idea of our framework is to reformulate all input sensory modalities, such as depth, thermal, and event data, as a single blind input X , while allowing the network to dynamically learn the modal nature, conditioned on which the most appropriate reasoning is accordingly assigned to improve the tracker’s robustness. This dynamic distribution is achieved through a mixture of experts design combined with a classification loss. Similar to the current mainstream target tracking paradigm, we input both the template and the search region, along with their associated multi-modal patches, into the network simultaneously to locate the target object.

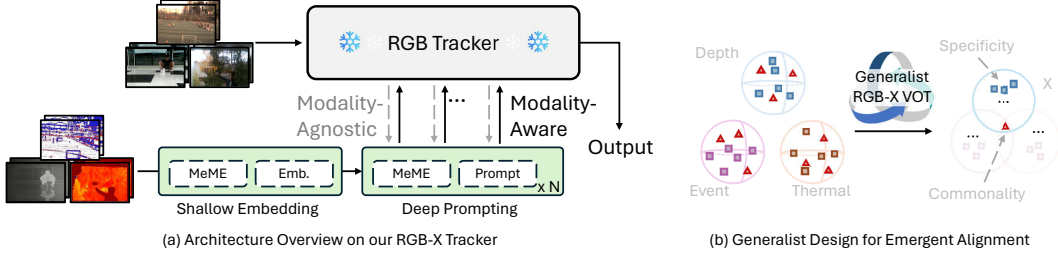


Figure 2: **Architecture:** Our XTrack leverages a Mixture of Modal Experts (MeME, see Sec.3.1 & Fig. 3) to bind all the modalities into a shared latent space, while without losing the modal-specific clues. Such a design naturally creates emergent alignment and enables joint benefit across modalities, while only paired RGB-X data are available during training.

3.1 Mixture of Modal Experts (MeME)

Basic Architecture: To align all the modalities, we employ a **Mixture of Modal Experts** (MeME). MeME operates on two key principles: (a) assigning the most appropriate and specialized experts based on the input modality, and (b) isolating the shared experts that are common across all modal inputs to facilitate cross-modal alignment and reasoning. By jointly incorporating both specialized and shared experts, MeME allows for the exploration of modal-specific clues with finer granularity thanks to the reduced redundancy within each specialized expert, and ensures emergent alignment across modalities, even when trained solely on paired data. An overview can be found in Fig. 2.

3.1.1 Routing among Specialized Experts with Multi-Label Classification Loss

In designing routing experts, we segment them into finer granularity to achieve higher specialization. While existing MoE networks primarily balance the input information for each expert, they often lack clearly defined roles for individual experts. This is particularly important in our modal setting, where the distinct modal features necessitate experts from different domains for appropriate reasoning.

To achieve this, our MeME starts by taking a pair of downstream modal features as input, compromising template modal input $T_x \in \mathbb{R}^{3 \times H_t \times W_t}$ and search region in the modal input $S_x \in \mathbb{R}^{3 \times H_s \times W_s}$. These patches are initially segmented and subsequently flattened into sequences of patch vectors, specifically $T_p \in \mathbb{R}^{N_t \times (3 \cdot P^2)}$ and $S_p \in \mathbb{R}^{N_s \times (3 \cdot P^2)}$, where $P \times P$ defines the spatial extent of each individual patch. The quantities N_t and N_s , calculated as $N_t = \frac{H_t W_t}{P^2}$ and $N_s = \frac{H_s W_s}{P^2}$, respectively, signify the count of patches pertaining to the template and search regions from the modal input. Following this transformation, a learnable linear projection layer $proj$ is utilized to map the patch sequences T_p and S_p into a D -dimensional latent space. These sequences are then concatenated, to meet the tracking specificity, and form O_x for subsequent processing and analysis:

$$O_x = concat(proj(T_p), proj(S_p)). \quad (1)$$

Therefore, the routed output is as follows:

$$y = \sum_{i \in top_k} p_i(O_x) \epsilon_i(O_x), \quad (2)$$

where we adopt top_k experts for routing the images, p_i is the probability, and ϵ_i is the expert.

Classification Loss: For the modality-aware specialization, during training, we employ a multi-class loss to constrain the data that each expert can process. Given a collection M of modalities, indexed by n , denoted as $m_{n=1}^{|M|}$. We introduce a mapping function $h : M \rightarrow \epsilon$ such that each modality m_n is associated with several particular experts $\epsilon_i \in \epsilon$, which ideally are not shared from one modality to another. The auxiliary loss \mathcal{L}_{moe} is computed using a binary cross-entropy loss, comparing the logits p_i (representing the probability of selecting experts) with the labels $h(m_n)$ (indicating the target expert for tokens from modality m_n). The expression for \mathcal{L}_{moe} is formulated as follows:

$$\mathcal{L}_{moe} = - \sum_{n=1}^{|M|} \sum_{i=1}^{|\epsilon|} 1\{h(m_n) = i\} \log p_i(O_x), \quad (3)$$

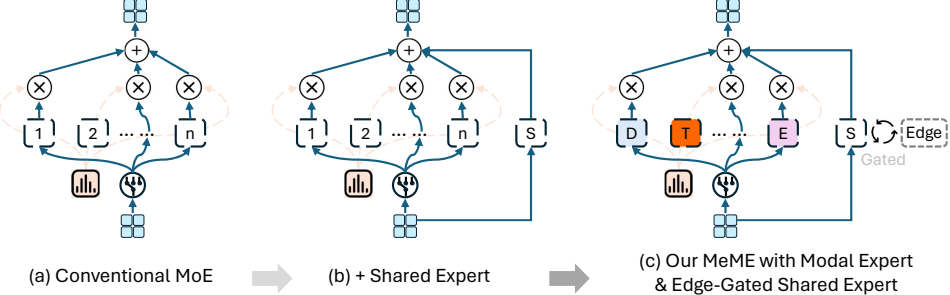


Figure 3: **Mixture of Modal Experts (MeME)**: MoE has demonstrated significant advancements recently. Recent work [9] has further leveraged shared experts to reduce redundancy. However, it remains unclear which expert learns what, due to the implicit learning setting. In contrast, we make the learning protocol explicit by assigning specific experts to particular modal inputs. Additionally, we enhance the shared expert model with inductive edge bias, increasing efficiency when dealing with relatively limited downstream data.

where $p_i(O_x)$ is the probability, $1_{h(m_n)=i}$ is the indicator function that equals to 1 if $h(m_n) = i$ and 0 otherwise, and $|\epsilon|$ is the cardinality of the set of experts ϵ .

Expert Balance Loss: To ensure a better distribution of modalities, we also use a balance loss compromising two parts: the importance loss \mathcal{L}_{ExpImp} and the loading loss $\mathcal{L}_{ExpLoad}$. We consider a norm distribution denoted as $\mathcal{N}(0, \sigma^2 \mathbf{I})$, where the standard deviation σ is defined as the ratio of gate noise to the number of experts $|\epsilon|$. The cumulative distribution function (CDF) of this normal distribution is denoted by $\Phi(\cdot)$.

For the load $Load_i$ of expert e_i , we evaluate the CDF at the probabilities $p_i(O_x)$, represented as $\Phi(p_i(O_x))$, and sum these values over all inputs O_x in a single mini-batch. The load loss $\mathcal{L}_{ExpLoad}$ is then defined as:

$$\mathcal{L}_{ExpLoad} = \frac{\text{Var}(Load)}{\text{Mean}(Load)^2}; \quad Load_i = \sum_{O_x \in batch} \Phi(p_i(O_x)). \quad (4)$$

Here, $Load_i$ represents the number of assignments allocated to expert e_i . Similarly, we obtain the importance loss \mathcal{L}_{ExpImp} without considering the CDF by:

$$\mathcal{L}_{ExpImp} = \frac{\text{Var}(Imp)}{\text{Mean}(Imp)^2}; \quad Imp_i = \sum_{O_x \in batch} p_i(O_x). \quad (5)$$

Hence, our balance loss $\mathcal{L}_{balance}$ is calculated by:

$$\mathcal{L}_{balance} = \mathcal{L}_{ExpImp} + \mathcal{L}_{ExpLoad}. \quad (6)$$

Finally, during training and on top of conventional tracking, our model additionally leverage both classification loss and balance loss to achieve our targeted generalist setting:

$$\mathcal{L}_{generalist} = \mathcal{L}_{moe} + \lambda \cdot \mathcal{L}_{balance}, \quad (7)$$

where λ is the proportion hyperparameter.

3.2 Efficient Expertized Reasoning and Gathering

Experts with Low-Rank Reasoning: The goal of each specialized expert is to project the input feature into a dedicated space for further processing. Inspired by recent successes in tuning large language models (LLMs), we aim to enhance efficiency by mitigating low-rank feature decomposition and reconstruction. Specifically, we project each input token with channel c to the significantly lower dimensional latent space k ($k \ll c$). This approach preserves the principal features while reducing computational cost, making the learning feasible on a single 24GB GPU.

Assume that our router decomposes the mixed modal input M into subset features m_n . Their respective k_{th} low-rank matrices m_{nk} , are approximated by:

$$m_{nk} = \epsilon_n(m_n), \quad (8)$$

where ϵ_n mimicks the low-rank projection for feature transformation. Note that all the ϵ_n structures are identical but without weight sharing, allowing for distinct reasoning.

Edge Guided Shared Expert: Simultaneously, we compute the shared low-rank matrix m_s from the shared expert ϵ_s . However, we believe that for the shared expert, a single projection through implicit learning might not be sufficient, especially when the training data size is relatively small compared to that used for training large foundation models. Therefore, we think it is necessary to incorporate additional human prior knowledge to guide the shared learning process. Since the objective is to find commonalities, we believe that high frequency is a naturally shared feature among these modalities, typically manifesting

In fact, event cameras naturally capture high-frequency temporal changes, recording events whenever there is a change in the scene. This is particularly useful for detecting rapid movements and transitions, leading to a denser distribution of event spikes around object boundaries. Similarly, spatial frequency in depth images refers to geometrical changes, often correlating with sharp edges. In thermal images, frequency can relate to the spatial variation of temperature. Areas with high spatial frequency changes in thermal readings often indicate edges where materials with different thermal properties meet. Therefore, we incorporate the additional edge clues as an inductive bias for shared expert reasoning.

Technically, we incorporate the shared low-rank projection with an additional gating module. Let m_{sk} be the shared low-rank feature, the meta-architecture is formulated as:

$$X = \text{Norm}(m_{sk}), \quad (9)$$

$$\text{Out} = (\sigma(\text{EdgeMixer}(XW_1)) \cdot XW_2)W_3 + m_{sk},$$

where $Norm()$ denotes the conventional normalization; $EdgeMixer()$ refers to the module responsible for conducting token mixing. Technically, we begin by transferring the token to a 2D feature form and then apply convolution to enable interaction between neighboring tokens. Unlike previous approaches, in our case, we additionally initialize the convolution with a Laplacian Filter, incorporating edge priors while remaining open to discovering more meaningful and learnable shared features. W_1, W_2, W_3 represent learnable parameters within the low-rank latent space. A graphical illustration of this process can be found in Fig. 4.

Fusion of Expertized Tokens: The next step aims for fusing previously separately reasoned tokends together into a global low-rank matrix M_k . It should contain both modality-specific and modality-shared clues. Technically, we develop a shringkage fusion design, where we first concatenate m_{nk} together batch-wise. Then, we learn a joint low-rank approximation from the whole batch, which is further incorporating with the shared matrix m_s . This pipeline can be expressed as follows:

$$M_k = ([m_{nk}]W_4 + m_{sk})W_5, \quad (10)$$

where $[\cdot]$ is the batch combination and W_4, W_5 are low-rank learnable parameters.

3.3 Modal Prompting

Finally, we aim to prompt the RGB token obtained from the frozen RGB foundation tracker and transform them to be modality-aware, making them more suitable for downstreaming and challenging cases. Following the same idea, we first project the RGB token into the low-rank space I_k . Then, we use approximated modal low-rank matrix M_k from Eq. 10 to prompt I_k . Our motivation is use the modality clues as a gating module to improve the RGB feature modeling. Specifically, we have:

$$\begin{aligned} X_i &= \text{Norm}(I_k), \quad X_m = \text{Norm}(M_k), \\ \text{Out} &= ((X_i W_5 \cdot \sigma(X_m W_6)) W_7 + I_k) W_8, \end{aligned} \quad (11)$$

where $TokenMixer()$ refers to learnable 2D convolution and W_5, W_6, W_7 are the learning parameters in the low-rank space, where W_8 projects the prompted token back to the initial embedding space.

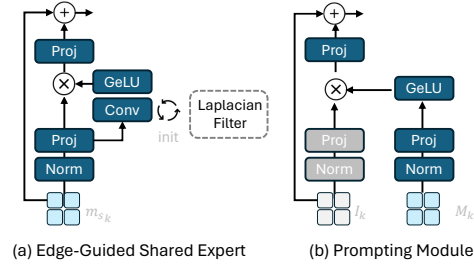


Figure 4: Details on experts and prompts.

Table 1: State-of-the-art comparison on DepthTrack[51], LasHeR[32], and VisEvent[45]. The best three results are shown in **red**, **blue**, and **green** fonts.

Method	Type	DepthTrack [51]			LasHeR [32]		VisEvent [45]	
		F-score(\uparrow)	Re(\uparrow)	Pr(\uparrow)	PR(\uparrow)	SR(\uparrow)	Precision(\uparrow)	Success(\uparrow)
XTrack	Generalist	59.7	59.7	59.8	65.5	52.5	75.6	59.1
UnTrack [47]	Unified but with prior knowledge	61.0	61.0	61.0	64.6	51.3	75.5	58.9
ViPT [66]	Depth-Specific Param.	59.4	59.6	59.2	-	-	-	-
ViPT [66]	Thermal-Specific Param.	-	-	-	65.1	52.5	-	-
ViPT [66]	Event-Specific Param.	-	-	-	-	-	75.8	59.2
ProTrack [53]	Depth-Specific Param.	57.8	57.3	58.3	-	-	-	-
ProTrack [53]	Thermal-Specific Param.	-	-	-	53.8	42.0	-	-
ProTrack [53]	Event-Specific Param.	-	-	-	-	-	63.2	47.1
SPT [67]	Depth-Specific Model	53.8	54.9	52.7	-	-	-	-
DeT [51]	Depth-Specific Model	53.2	50.6	56.0	-	-	-	-
DDiMP [26]	Depth-Specific Model	48.5	46.9	50.3	-	-	-	-
ATCAIS [26]	Depth-Specific Model	47.6	45.5	50.0	-	-	-	-
MacNet [57]	Thermal-Specific Model	-	-	-	48.2	35.0	-	-
DAFNet [14]	Thermal-Specific Model	-	-	-	44.8	31.1	-	-
mfDiMP [59]	Thermal-Specific Model	-	-	-	44.7	34.3	-	-
FANet [68]	Thermal-Specific Model	-	-	-	44.1	30.9	-	-
SGT [30]	Thermal-Specific Model	-	-	-	32.7	23.2	-	-
TransT_E [7]	Event-Specific Model	-	-	-	-	-	65.0	47.4
PrDiMP_E [11]	Event-Specific Model	-	-	-	-	-	64.4	45.3
VITAL_E [40]	Event-Specific Model	-	-	-	-	-	64.9	41.5
Stark_E [50]	Event-Specific Model	-	-	-	-	-	61.2	44.6
SiamCAR [17]	Event-Specific Model	-	-	-	-	-	59.9	42.0

4 Experiments

4.1 Implementation Details

We adopt [54] as RGB foundation by freezing the parameters. To train our XTrack, we only train our shallow embedding and deep prompts, as shown in Fig.2. We set the batch size to 64, with a learning rate of 0.0004, training for 60 epochs. The learning rate is decreased by a factor of 10 after 48 epochs. In addition to the object tracking loss shared with the RGB Tracker, we incorporate a loss that guides MoE expert balance and specialization of modality-specific experts, as detailed in Sec 3.1.1.

Regarding dataset selection, we utilize DepthTrack for RGB-D sequences, LasHeR for RGB-T sequences, and VisEvent for RGB-E sequences. Previous well-established modality-tailored works [66, 53, 20, 21], we train our model by inputting data from all three datasets simultaneously.

We want to highlight that only one RGB-X pair (i.e. RGB-depth, **or** RGB-thermal, **or** RGB-event) is available at a time, which makes our problem setting challenging.

4.2 Within Distribution Evaluation

We first analyze the within distribution performances, while our models are jointly trained on DepthTrack [51], LasHeR [32], and VisEvent [45], and tested on the dedicated testing set from each modality. Notably, we compare our XTrack with three groups of competitors: 1) specific models only for tackling one dataset, e.g., SPT [67], DeT [51], DDiMP [26], ATCAIS [25], MacNet [57], DAFNet [14], and so on; 2) single model but has different sets of parameters for different datasets: ViPT [66] and ProTrack [29]; 3) Unified model but requires modality prior: UnTrack [47]. The comparison results are summarized in Tab. 1. Note that our model uses **a single parameter set** and treats all modalities equally as a **blind X** input, while all other methods require prior knowledge of the modal nature and most of them adopt a parameter- and/or model-specific design. The detailed analysis of each dataset is as follows.

DepthTrack: DepthTrack [51] is a comprehensive long-distance dataset comprising 50 sets of test video sequences. We evaluate the accuracy of various trackers using F-score, Recall (Re), and Precision (Pr) metrics. From the results, we observe that: 1) our XTrack outperforms all the specific models proposed for the DepthTrack dataset, as well as the unified models with different sets of parameters. This demonstrates the effectiveness of our method; 2) UnTrack performs slightly better than our method. However, given that UnTrack uses more information, specifically the modality types, this slight disadvantage is acceptable.

Table 2: Overall performance on RGBT234 dataset [31]. Our Generalist model sets new SOTA records.

	Thermal-Specific Parameters									Generalist XTrack (ours)
	mfDiMP [59]	SGT [30]	DAFNet [14]	FANet [68]	MaCNet [57]	CMPP [43]	APFNet [48]	ProTrack [53]	ViPT [66]	
MPR(\uparrow)	64.6	72.0	79.6	78.7	79.0	82.3	82.7	79.5	83.5	84.8
MSR(\uparrow)	42.8	47.2	54.4	55.3	55.4	57.5	57.9	59.9	61.7	62.2

Table 3: Overall performance on VOT-RGBD2022 dataset [28].

	Depth-Specific Parameters								Generalist XTrack (ours)
	DRefine [27]	Stark_d [50]	DMTracker [13]	DeT [51]	SBT_D [49]	SPT [67]	ProTrack [53]	ViPT [66]	
EAO(\uparrow)	59.2	64.7	65.8	65.7	70.8	65.1	65.1	72.1	71.4
Accuracy(\uparrow)	77.5	80.3	75.8	76.0	80.9	79.8	80.1	81.6	81.2
Robustness(\uparrow)	76.0	79.8	85.1	84.5	86.4	85.1	80.2	87.1	86.5

LasHeR The LasHeR [32] dataset is a large-scale, high-quality dataset comprising 245 test sequences. We evaluate the performance of trackers using precision (Pr) and success plots (SR). Notably, XTrack achieves SOTA on this dataset clearly outperforming all the competitors even including the most competitive UnTrack[47] and ViPT[66]. This enhancement well validates the advantages of our method: take advantage of both the modality-shared and modality-specific features.

VisEvent VisEvent[45] is a large-scale dataset containing RGB images and event data for object tracking, comprising 320 test sequences. We use precision (PR) and success plots (SR) to evaluate the performance of different trackers. Results show that our XTrack outperforms the UnTrack[47] and obtains very comparable to the ViPT[66] again indicating our effectiveness. In addition, we highlight that our inference stage is quite efficient due to the MeME design, only activating the selected experts.

4.3 Out-of-Distribution Generalization

To further assess the generalization performance of our model, we also conducted experiments on two out-of-distribution datasets including RGBT234 and RGBD2022.

RGBT234: The RGBT234[31] dataset is a comprehensive video dataset, including 234 sequences videos for test, encompassing a variety of environmental challenges, including rainy conditions, nighttime scenes, and extreme weather scenarios ranging from cold to hot. Results in Tab. 2 show that our Xtrack gains clear improvements compared to other methods even in unseen sequences.

VOT-RGBD2022: The VOT-RGBD2022[28] dataset, comprising 127 video sequences, is the latest RGB-D object tracking benchmark. We evaluate the performance of our tracking model using accuracy, robustness, and expected average overlap (EAO). Results are given in Tab. 3. Although our model’s performance is not as strong as desired, primarily due to the limited RGB-D training data (150 sequences) compared to RGB-E with 500 sequences and RGB-T datasets with 979 sequences. However, as a generalist model, XTrack still demonstrates commendable overall performance.

4.4 Ablation Study

We conduct ablation studies on the DepthTrack dataset.

Table 4: Ablation studies on the MoME by gradually removing the key components. The performance deteriorates as expected.

Model	Shared Experts	Modality-Specific Experts	DepthTrack		
			F-score	Re	Pr
XTrack	✓	✓	59.7	59.7	59.8
		✓	59.0	59.2	58.8
	✓		57.8	57.9	57.8

Table 5: Ablation study of number of modality-specific experts.

Nbr.	F-score	Re	Pr
1	56.6	56.6	56.6
2	59.7	59.7	59.8
3	57.5	57.9	57.1

Shared Experts In the design of MeME, we use a shared expert to capture modality-shared features across different modalities. To evaluate the impact of this shared expert, we removed it from MeME, making the output of each MeME consist solely of modality-specific experts. As shown in Tab. 4, we found that removing the shared experts resulted in a 0.7% decrease in F-score. This indicates that the shared experts successfully capture commonalities across modalities. In addition, removing the shared expert may lead to redundancy in the modality-specialized experts, reducing their effectiveness and hence leading to a performance drop. Such an observation joins the conclusion from the previous work [9]. It is worthy noting that our whole model only requires around 100M parameters, with only +8M parameters compared to our RGB baseline. The 8M parameters are used by all the experts, in total 8 experts in our final settings. Hence, the shared experts only represent around 1M parameters, while enabling significant performance improvement.

Modality Specific Experts In addition to the shared expert, our MeME also includes modality-specific experts to capture unique information from each modality. As shown in Tab. 4, we removed the modality-specific experts and processed all modalities using a single expert. We observed a performance degradation, with a 1.9% drop in the F-score. The performance decline produced by removing the modality-specific experts indicates the effectiveness of our decomposition of modality-shared and modality-specific features. When there is no modality-specific experts, all the experts are treated equally, losing the identification such as geometry from depth, motion from event, or temperature from Thermal. Our modality-specific design enables us to effectively model each modality’s characteristics and make the different modalities benefit from each other.

Number of Experts We also explored the impact of the number of modality-specific experts used for each modality on the results. We set the number of experts specific to each modality to 1, where each modality uses a single expert. We used cross-entropy loss to force each expert to learn modality-specific information. Additionally, we set the number of experts corresponding to each modality to 2 and 3, as shown in Tab. 5, transforming the classification loss to a multi-label one. The experimental results indicate that using two modality-specific experts yields the best performance. If each modality has only one dedicated expert, the feature representation is constrained. If each modality has three experts, internal conflicts among the modality-specific experts arise, negatively impacting the performance of the model.

We believe that the number of expert is also correlated to the expert design. Since we leverage a low-rank architecture, while being efficient, this limits the network’s capability of deeply explore the more meaningful clues. On the other hand, this can also be impacted by the choice on the baseline tracker, which somehow limits the performance upbound. Finally, the training data size can also have an influence here. We believe that with more data, we shall be able to have better performance with more experts.

5 Conclusion

In conclusion, we have made significant strides in the field of RGB-X video object tracking, aiming to develop a generalist tracker that better aligns with AGI expectations. Our proposed tracker, termed as XTrack, which incorporates a novel mixture of model experts (MeME) and a dynamic router, can handle any modality as input without requiring prior knowledge during inference. Extensive experimental results have validated the effectiveness of our method, demonstrating its robustness and efficiency in various tracking scenarios including in-distribution and out-of-distribution cases. These contributions pave the way for future advancements in creating more robust and generalizable tracking models. Our experiments are reported in the well tested benchmark datasets, where an exhaustive comparison on different fronts can also be found. Furthermore, the well utilized RGB-only dataset followed by the inclusion of the additional modalities of the RGB-X shows a way of adding other modalities in the similar fashion, without requiring large modality specific datasets anymore.

Limitations and social impact. The current performance of the proposed generalist tracker is not always competitive against the specialist models. Furthermore, while being blind during inference, the current method still requires the modalities to be known during the training. Like other deep learning algorithms, our method needs to be trained on large-scale datasets to perform well. The object tracking has widespread use, and we support its use only in the socially beneficial cases.

References

- [1] H. Akbari, D. Kondratyuk, Y. Cui, R. Hornung, H. Wang, and H. Adam. Alternating gradient descent and mixture-of-experts for integrated multimodal perception. *Advances in Neural Information Processing Systems*, 36, 2024.
- [2] M. Awais, M. Naseer, S. Khan, R. M. Anwer, H. Cholakkal, M. Shah, M.-H. Yang, and F. S. Khan. Foundational models defining a new era in vision: A survey and outlook. *arXiv preprint arXiv:2307.13721*, 2023.
- [3] B. Cao, J. Guo, P. Zhu, and Q. Hu. Bi-directional adapter for multimodal tracking. In *Proceedings of the AAAI Conference on Artificial Intelligence*, volume 38, pages 927–935, 2024.
- [4] R. Caruana. Multitask learning. *Machine learning*, 28:41–75, 1997.
- [5] S. Chen, P. Sun, Y. Song, and P. Luo. Diffusiondet: Diffusion model for object detection. In *Proceedings of the IEEE/CVF International Conference on Computer Vision*, pages 19830–19843, 2023.
- [6] T. Chen, L. Li, S. Saxena, G. Hinton, and D. J. Fleet. A generalist framework for panoptic segmentation of images and videos. In *Proceedings of the IEEE/CVF International Conference on Computer Vision*, pages 909–919, 2023.
- [7] X. Chen, B. Yan, J. Zhu, D. Wang, X. Yang, and H. Lu. Transformer tracking. In *Proceedings of the IEEE/CVF conference on computer vision and pattern recognition*, pages 8126–8135, 2021.
- [8] Z. Chen, B. Zhong, G. Li, S. Zhang, R. Ji, Z. Tang, and X. Li. Siamban: Target-aware tracking with siamese box adaptive network. *IEEE Transactions on Pattern Analysis and Machine Intelligence*, 45(4):5158–5173, 2022.
- [9] D. Dai, C. Deng, C. Zhao, R. Xu, H. Gao, D. Chen, J. Li, W. Zeng, X. Yu, Y. Wu, et al. Deepseek-moe: Towards ultimate expert specialization in mixture-of-experts language models. *arXiv preprint arXiv:2401.06066*, 2024.
- [10] M. Danelljan, G. Bhat, F. S. Khan, and M. Felsberg. Atom: Accurate tracking by overlap maximization. In *Proceedings of the IEEE/CVF conference on computer vision and pattern recognition*, pages 4660–4669, 2019.
- [11] M. Danelljan, L. V. Gool, and R. Timofte. Probabilistic regression for visual tracking. In *Proceedings of the IEEE/CVF conference on computer vision and pattern recognition*, pages 7183–7192, 2020.
- [12] J. Devlin, M.-W. Chang, K. Lee, and K. Toutanova. Bert: Pre-training of deep bidirectional transformers for language understanding. *arXiv preprint arXiv:1810.04805*, 2018.
- [13] S. Gao, J. Yang, Z. Li, F. Zheng, A. Leonardis, and J. Song. Learning dual-fused modality-aware representations for rgbd tracking. In *European Conference on Computer Vision*, pages 478–494. Springer, 2022.
- [14] Y. Gao, C. Li, Y. Zhu, J. Tang, T. He, and F. Wang. Deep adaptive fusion network for high performance rgbt tracking. In *2019 IEEE/CVF International Conference on Computer Vision Workshop (ICCVW)*, pages 91–99, 2019. doi: 10.1109/ICCVW.2019.00017.
- [15] R. Girdhar, A. El-Nouby, Z. Liu, M. Singh, K. V. Alwala, A. Joulin, and I. Misra. Imagebind: One embedding space to bind them all. In *Proceedings of the IEEE/CVF Conference on Computer Vision and Pattern Recognition*, pages 15180–15190, 2023.
- [16] J. Gu, Z. Han, S. Chen, A. Beirami, B. He, G. Zhang, R. Liao, Y. Qin, V. Tresp, and P. Torr. A systematic survey of prompt engineering on vision-language foundation models. *arXiv preprint arXiv:2307.12980*, 2023.
- [17] D. Guo, J. Wang, Y. Cui, Z. Wang, and S. Chen. Siamcar: Siamese fully convolutional classification and regression for visual tracking. In *Proceedings of the IEEE/CVF conference on computer vision and pattern recognition*, pages 6269–6277, 2020.
- [18] B. He, H. Li, S. Wu, D. Wang, Z. Zhang, Q. Dong, C. Xu, and F. Gao. Fast-dynamic-vision: Detection and tracking dynamic objects with event and depth sensing. In *2021 IEEE/RSJ International Conference on Intelligent Robots and Systems (IROS)*, pages 3071–3078. IEEE, 2021.
- [19] J. F. Henriques, R. Caseiro, P. Martins, and J. Batista. High-speed tracking with kernelized correlation filters. *IEEE transactions on pattern analysis and machine intelligence*, 37(3):583–596, 2014.

[20] L. Hong, S. Yan, R. Zhang, W. Li, X. Zhou, P. Guo, K. Jiang, Y. Chen, J. Li, Z. Chen, et al. Onetracker: Unifying visual object tracking with foundation models and efficient tuning. *arXiv preprint arXiv:2403.09634*, 2024.

[21] X. Hou, J. Xing, Y. Qian, Y. Guo, S. Xin, J. Chen, K. Tang, M. Wang, Z. Jiang, L. Liu, et al. Sd-strack: Self-distillation symmetric adapter learning for multi-modal visual object tracking. *arXiv preprint arXiv:2403.16002*, 2024.

[22] T. Hui, Z. Xun, F. Peng, J. Huang, X. Wei, X. Wei, J. Dai, J. Han, and S. Liu. Bridging search region interaction with template for rgb-t tracking. In *Proceedings of the IEEE/CVF Conference on Computer Vision and Pattern Recognition*, pages 13630–13639, 2023.

[23] Y. Jain, H. Behl, Z. Kira, and V. Vineet. Damex: Dataset-aware mixture-of-experts for visual understanding of mixture-of-datasets. *Advances in Neural Information Processing Systems*, 36, 2024.

[24] H. Kiani Galoogahi, A. Fagg, and S. Lucey. Learning background-aware correlation filters for visual tracking. In *Proceedings of the IEEE international conference on computer vision*, pages 1135–1143, 2017.

[25] M. Kristan, A. Leonardis, J. Matas, M. Felsberg, R. Pflugfelder, J.-K. Kämäriäinen, M. Danelljan, L. Č. Zajc, A. Lukežič, O. Drbohlav, et al. The eighth visual object tracking vot2020 challenge results. In *Computer Vision–ECCV 2020 Workshops: Glasgow, UK, August 23–28, 2020, Proceedings, Part V 16*, pages 547–601. Springer, 2020.

[26] M. Kristan, A. Leonardis, J. Matas, M. Felsberg, R. Pflugfelder, J.-K. Kämäriäinen, M. Danelljan, L. Č. Zajc, A. Lukežič, O. Drbohlav, et al. The eighth visual object tracking vot2020 challenge results. In *Computer Vision–ECCV 2020 Workshops: Glasgow, UK, August 23–28, 2020, Proceedings, Part V 16*, pages 547–601. Springer, 2020.

[27] M. Kristan, J. Matas, A. Leonardis, M. Felsberg, R. Pflugfelder, J.-K. Kämäriäinen, H. J. Chang, M. Danelljan, L. Č. Zajc, A. Lukežič, et al. The ninth visual object tracking vot2021 challenge results. In *Proceedings of the IEEE/CVF international conference on computer vision*, pages 2711–2738, 2021.

[28] M. Kristan, A. Leonardis, J. Matas, M. Felsberg, R. Pflugfelder, J.-K. Kämäriäinen, H. J. Chang, M. Danelljan, L. Č. Zajc, A. Lukežič, et al. The tenth visual object tracking vot2022 challenge results. In *European Conference on Computer Vision*, pages 431–460. Springer, 2022.

[29] B. Lester, R. Al-Rfou, and N. Constant. The power of scale for parameter-efficient prompt tuning. *arXiv preprint arXiv:2104.08691*, 2021.

[30] C. Li, N. Zhao, Y. Lu, C. Zhu, and J. Tang. Weighted sparse representation regularized graph learning for rgb-t object tracking. In *Proceedings of the 25th ACM international conference on Multimedia*, pages 1856–1864, 2017.

[31] C. Li, X. Liang, Y. Lu, N. Zhao, and J. Tang. Rgb-t object tracking: Benchmark and baseline. *Pattern Recognition*, 96:106977, 2019.

[32] C. Li, W. Xue, Y. Jia, Z. Qu, B. Luo, J. Tang, and D. Sun. Lasher: A large-scale high-diversity benchmark for rgbt tracking. *IEEE Transactions on Image Processing*, 31:392–404, 2021.

[33] H. Li, J. Zhu, X. Jiang, X. Zhu, H. Li, C. Yuan, X. Wang, Y. Qiao, X. Wang, W. Wang, et al. Uni-perceiver v2: A generalist model for large-scale vision and vision-language tasks. In *Proceedings of the IEEE/CVF Conference on Computer Vision and Pattern Recognition*, pages 2691–2700, 2023.

[34] V. Likhoshsterstov, A. Arnab, K. Choromanski, M. Lucic, Y. Tay, A. Weller, and M. Dehghani. Polyvit: Co-training vision transformers on images, videos and audio. *arXiv preprint arXiv:2111.12993*, 2021.

[35] Z. Liu, Y. Lin, Y. Cao, H. Hu, Y. Wei, Z. Zhang, S. Lin, and B. Guo. Swin transformer: Hierarchical vision transformer using shifted windows. In *Proceedings of the IEEE/CVF international conference on computer vision*, pages 10012–10022, 2021.

[36] J. Lu, C. Clark, R. Zellers, R. Mottaghi, and A. Kembhavi. Unified-io: A unified model for vision, language, and multi-modal tasks. In *The Eleventh International Conference on Learning Representations*, 2022.

[37] M. Moor, O. Banerjee, Z. S. H. Abad, H. M. Krumholz, J. Leskovec, E. J. Topol, and P. Rajpurkar. Foundation models for generalist medical artificial intelligence. *Nature*, 616(7956):259–265, 2023.

[38] B. Mustafa, C. Riquelme, J. Puigcerver, R. Jenatton, and N. Houlsby. Multimodal contrastive learning with limoe: the language-image mixture of experts. *Advances in Neural Information Processing Systems*, 35:9564–9576, 2022.

[39] C. Riquelme, J. Puigcerver, B. Mustafa, M. Neumann, R. Jenatton, A. Susano Pinto, D. Keysers, and N. Houlsby. Scaling vision with sparse mixture of experts. *Advances in Neural Information Processing Systems*, 34:8583–8595, 2021.

[40] Y. Song, C. Ma, X. Wu, L. Gong, L. Bao, W. Zuo, C. Shen, R. W. Lau, and M.-H. Yang. Vital: Visual tracking via adversarial learning. In *Proceedings of the IEEE conference on computer vision and pattern recognition*, pages 8990–8999, 2018.

[41] S. Subramanian, P. Harrington, K. Keutzer, W. Bhimji, D. Morozov, M. W. Mahoney, and A. Gholami. Towards foundation models for scientific machine learning: Characterizing scaling and transfer behavior. *Advances in Neural Information Processing Systems*, 36, 2024.

[42] H. Touvron, T. Lavigra, G. Izacard, X. Martinet, M.-A. Lachaux, T. Lacroix, B. Rozière, N. Goyal, E. Hambro, F. Azhar, et al. Llama: Open and efficient foundation language models. *arXiv preprint arXiv:2302.13971*, 2023.

[43] C. Wang, C. Xu, Z. Cui, L. Zhou, T. Zhang, X. Zhang, and J. Yang. Cross-modal pattern-propagation for rgb-t tracking. In *Proceedings of the IEEE/CVF Conference on computer vision and pattern recognition*, pages 7064–7073, 2020.

[44] W. Wang, Z. Chen, X. Chen, J. Wu, X. Zhu, G. Zeng, P. Luo, T. Lu, J. Zhou, Y. Qiao, et al. Visionllm: Large language model is also an open-ended decoder for vision-centric tasks. *Advances in Neural Information Processing Systems*, 36, 2024.

[45] X. Wang, J. Li, L. Zhu, Z. Zhang, Z. Chen, X. Li, Y. Wang, Y. Tian, and F. Wu. Visevent: Reliable object tracking via collaboration of frame and event flows. *IEEE Transactions on Cybernetics*, pages 1–14, 2023.

[46] X. Wang, W. Wang, Y. Cao, C. Shen, and T. Huang. Images speak in images: A generalist painter for in-context visual learning. In *Proceedings of the IEEE/CVF Conference on Computer Vision and Pattern Recognition*, pages 6830–6839, 2023.

[47] Z. Wu, J. Zheng, X. Ren, F.-A. Vasluiianu, C. Ma, D. P. Paudel, L. Van Gool, and R. Timofte. Single-model and any-modality for video object tracking. *arXiv preprint arXiv:2311.15851*, 2023.

[48] Y. Xiao, M. Yang, C. Li, L. Liu, and J. Tang. Attribute-based progressive fusion network for rgbt tracking. In *Proceedings of the AAAI Conference on Artificial Intelligence*, volume 36, pages 2831–2838, 2022.

[49] F. Xie, C. Wang, G. Wang, Y. Cao, W. Yang, and W. Zeng. Correlation-aware deep tracking. In *Proceedings of the IEEE/CVF Conference on Computer Vision and Pattern Recognition*, pages 8751–8760, 2022.

[50] B. Yan, H. Peng, J. Fu, D. Wang, and H. Lu. Learning spatio-temporal transformer for visual tracking. In *Proceedings of the IEEE/CVF international conference on computer vision*, pages 10448–10457, 2021.

[51] S. Yan, J. Yang, J. Käpylä, F. Zheng, A. Leonardis, and J.-K. Kämäräinen. Depthtrack: Unveiling the power of rgbd tracking. In *Proceedings of the IEEE/CVF International Conference on Computer Vision*, pages 10725–10733, 2021.

[52] J. Yang, Z. Li, S. Yan, F. Zheng, A. Leonardis, J.-K. Kämäräinen, and L. Shao. Rgbd object tracking: An in-depth review. *arXiv preprint arXiv:2203.14134*, 2022.

[53] J. Yang, Z. Li, F. Zheng, A. Leonardis, and J. Song. Prompting for multi-modal tracking. In *Proceedings of the 30th ACM International Conference on Multimedia*, pages 3492–3500, 2022.

[54] B. Ye, H. Chang, B. Ma, S. Shan, and X. Chen. Joint feature learning and relation modeling for tracking: A one-stream framework. In *European Conference on Computer Vision*, pages 341–357. Springer, 2022.

[55] Y. Yuan. On the power of foundation models. In *International Conference on Machine Learning*, pages 40519–40530. PMLR, 2023.

[56] C. Zhang, L. Liu, Y. Cui, G. Huang, W. Lin, Y. Yang, and Y. Hu. A comprehensive survey on segment anything model for vision and beyond. *arXiv preprint arXiv:2305.08196*, 2023.

[57] H. Zhang, L. Zhang, L. Zhuo, and J. Zhang. Object tracking in rgbt videos using modal-aware attention network and competitive learning. *Sensors*, 20(2):393, 2020.

[58] J. Zhang, B. Dong, H. Zhang, J. Ding, F. Heide, B. Yin, and X. Yang. Spiking transformers for event-based single object tracking. In *CVPR*, 2022.

[59] L. Zhang, M. Danelljan, A. Gonzalez-Garcia, J. Van De Weijer, and F. Shahbaz Khan. Multi-modal fusion for end-to-end rgb-t tracking. In *Proceedings of the IEEE/CVF International conference on computer vision workshops*, pages 2252–2261, 2019.

[60] P. Zhang, J. Zhao, D. Wang, H. Lu, and X. Ruan. Visible-thermal uav tracking: A large-scale benchmark and new baseline. In *CVPR*, 2022.

[61] Y. Zhang, K. Gong, K. Zhang, H. Li, Y. Qiao, W. Ouyang, and X. Yue. Meta-transformer: A unified framework for multimodal learning. *arXiv preprint arXiv:2307.10802*, 2023.

[62] H. Zhao, D. Wang, and H. Lu. Representation learning for visual object tracking by masked appearance transfer. In *CVPR*, pages 18696–18705, 2023.

[63] J. Zhao, X. Zhang, and P. Zhang. A unified approach for tracking uavs in infrared. In *ICCV*, pages 1213–1222, 2021.

[64] X. Zhao, Y. Pang, W. Ji, B. Sheng, J. Zuo, L. Zhang, and H. Lu. Spider: A unified framework for context-dependent concept understanding. *arXiv preprint arXiv:2405.01002*, 2024.

[65] J. Zhu, Z. Chen, Z. Hao, S. Chang, L. Zhang, D. Wang, H. Lu, B. Luo, J.-Y. He, J.-P. Lan, et al. Tracking anything in high quality. *arXiv preprint arXiv:2307.13974*, 2023.

[66] J. Zhu, S. Lai, X. Chen, D. Wang, and H. Lu. Visual prompt multi-modal tracking. In *Proceedings of the IEEE/CVF Conference on Computer Vision and Pattern Recognition*, pages 9516–9526, 2023.

[67] X.-F. Zhu, T. Xu, Z. Tang, Z. Wu, H. Liu, X. Yang, X.-J. Wu, and J. Kittler. Rgbdlk: A large-scale dataset and benchmark for rgb-d object tracking. In *Proceedings of the AAAI Conference on Artificial Intelligence*, volume 37, pages 3870–3878, 2023.

[68] Y. Zhu, C. Li, J. Tang, and B. Luo. Quality-aware feature aggregation network for robust rgbt tracking. *IEEE Transactions on Intelligent Vehicles*, 6(1):121–130, 2020.

[69] Z. Zhu, J. Hou, and D. O. Wu. Cross-modal orthogonal high-rank augmentation for rgb-event transformer-trackers. In *ICCV*, pages 21988–21998, 2023.

Appendix

S.1 Selection of Experts

For each modality, we employ a multi-class loss on top of the router to ensure that each modality has its own dedicated experts. To validate the design, we visualize the distribution of different experts, as shown in Fig. 5. For ease of review, we take event dataset VisEvent [45] as an example. It can be seen that our router perfectly assign the event experts to analyze the input event data, with only a negligible small amount of misclassification in the shallow embedding space. Such a visualization validates our modality-aware multi-label classification loss and corresponds well to our initial motivation of assigning right experts to input.

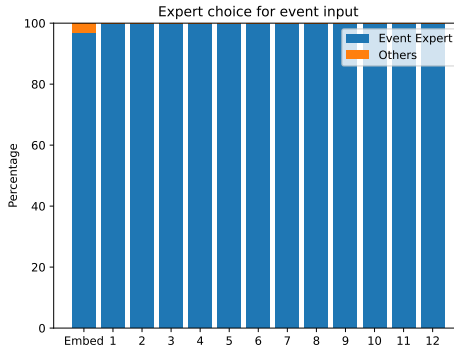


Figure 5: The selection of RGB-Event data, "embed" representing the selection of experts in the patch embedding layer.

S.2 Visualization results

In our main manuscript, we have shown that our XTrack has achieved overall best performance on the challenging RGBT234 [31] dataset. Here, we aim for a more in-depth analysis of the performances vis-a-vis sequences with different attributes. As shown in Fig. 6, the results show that our generalist and blind XTrack outperforms SOTA counterparts with thermal-specialized weight in various challenging scenarios, such as scale variation and camera moving. These sequences are typically the challenges that can be dealt by depth camera and event camera. Hence, our superior performance shows that our tracker can effectively leverage the cross-modal joint benefit with emergent alignments, even though depth and event are not naturally available in the RGB-T dataset.

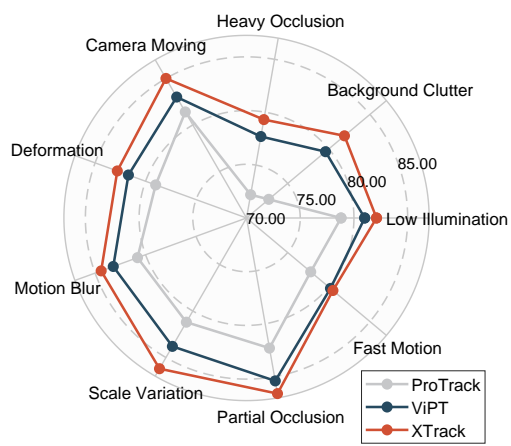


Figure 6: Performance of models under different attributes in RGB234 dataset.